

Tunable compression of template banks for fast gravitational wave detection and identification

Alvin J. K. Chua* and Jonathan R. Gair†
*Institute of Astronomy, University of Cambridge,
Madingley Road, Cambridge CB3 0HA, United Kingdom*

(Dated: November 10, 2018)

One strategy for reducing the computational cost of matched-filter searches for gravitational wave sources is to introduce a compressed basis for the waveform template bank in a grid-based search. In this paper, we propose and investigate several tunable compression schemes that slide between maximal sensitivity and maximal compression; these might be useful for the fast detection and identification of sources with moderate to high signal-to-noise ratios. Lossless compression schemes offer automatic identification of the signal upon detection, but their accuracy is significantly reduced in the presence of noise. A lossy scheme that uses a straightforward partition of the template bank is found to yield better detection and identification performance at the same level of compression.

PACS numbers: 04.80.Nn, 95.55.Ym, 95.75.Wx

I. INTRODUCTION

The first direct detections of gravitational waves (GWs) from astrophysical sources are expected to be made within the next few years by the ground-based interferometer network comprising Advanced LIGO [1] and Advanced Virgo [2]. These will be followed over the next two decades by detections of nanohertz GW sources using pulsar timing arrays [3], and of millihertz sources by the proposed space mission eLISA [4]. The search for GW signals in noisy data from such detectors—and the follow-up estimation of their source parameters—will be contingent upon reliable statistical analysis of the data.

Continuous GW signals from sources such as stellar-mass compact binary inspirals or massive black-hole binary mergers are typically weak compared to the detector noise in which they are embedded. The standard approach in GW data analysis is to correlate the detector data with a bank of waveform templates sampled from the parameter space of a waveform model, which allows signal-to-noise ratio (SNR) to be built up over the detector bandwidth. This correlation is essentially an inner product on the function space of finite-length time series; it must be evaluated numerically for each template, and carries the bulk of the computational cost in online GW searches [5, 6].

Various strategies exist to reduce the cost of evaluating inner products for GW detection and parameter estimation purposes. Some methods focus on making individual inner products computationally cheaper: this may be achieved across regions of parameter space through direct interpolation [7, 8], or more generally by using a reduced order quadrature [9, 10]. Other methods seek to reduce the number of required inner products: either by accelerating the convergence to correlation maxima in

a stochastic search [11–13], or through compressed-basis decomposition of the template bank in a grid search [14–16].

In a recently proposed method for evaluating fewer inner products in a grid search, binary labelling is used to define a compressed non-orthogonal basis that maximises compression losslessly (in the sense of perfect signal recovery without noise) [17]. This idea is fully general and admits a much larger compression rate than existing methods based on the eigenvalue structure of the template bank, but comes with significant penalties to detection sensitivity and identification accuracy. The method as presented also suffers from an arbitrarily asymmetric treatment of templates, as well as a restrictive level of compression that limits its practicality to high-SNR signals.

We propose in this paper several alternative compression schemes, both lossless and lossy, that subsume a symmetric-treatment version of the binary labelling method [17] as a particular case. These tunable schemes offer discrete transitions between zero and maximal compression, and may be used to trade performance for computational savings in a controlled manner. Apart from their fast detection and identification of moderate- to high-SNR sources, their generality and straightforward implementation also allow them to supplement existing grid-search methods, or to rapidly identify seed points for stochastic searches.

The general method of conic compression (i.e. defining a compressed basis through conic combinations of templates) is detailed in Sec. II. Three families of conic compression schemes are then proposed: a lossy scheme based on simple partitioning of the template bank, and two lossless schemes whose conic combinations are determined permutatively or by base representations of template labels. We calculate the optimal detection statistics for these schemes, and find that the standard maximum-overlap detection statistic is significantly suboptimal in the lossless case.

Sec. III compares the performance of our tunable com-

*Electronic address: ajkc3@ast.cam.ac.uk

†Electronic address: jgair@ast.cam.ac.uk

pression schemes under idealised conditions, i.e. assuming the GW signal is proportional to a single template in an orthogonal template bank. The lossy partition scheme is shown to outperform its lossless counterparts at the same level of compression, since the added structure in lossless methods tends to increase the generalised variance of the conic statistics. Furthermore, while the lossless schemes provide automatic identification of the signal upon detection, the identification accuracy falls off rapidly with compression in the presence of noise.

The orthogonality and single-template assumptions are lifted (separately) in Sec. IV for the partition scheme. Overall performance is seen to be highly partition-dependent in the case of a non-orthogonal template bank, although general strategies for pre-optimising the partition are available. For GW signals lying in a low-dimensional template subspace, the detection performance becomes more variable but is not significantly reduced.

II. COMPRESSION SCHEMES

In the standard GW data analysis framework, data from a detector may be written as the time series

$$\mathcal{X}(t) = \mathcal{S}(t) + \mathcal{N}(t), \quad (1)$$

where the GW signal $\mathcal{S}(t)$ is a deterministic function and the (additive) detector noise $\mathcal{N}(t)$ is a Gaussian and stationary stochastic process.

Matched filtering involves passing the data through some GW template filter $\mathcal{F}(t)$ via convolution, which defines an inner product on the function space of finite-length time series. This inner product is given by

$$\langle \mathcal{X} | \mathcal{F} \rangle = \int_{-\infty}^{\infty} \frac{\tilde{\mathcal{X}}(f) \tilde{\mathcal{F}}^*(f)}{S_{\mathcal{N}}(f)} df, \quad (2)$$

where $S_{\mathcal{N}}(f)$ is the two-sided spectral density of the detector noise. Since $\mathcal{N}(t)$ is stationary, $S_{\mathcal{N}}(f)$ is simply the Fourier transform of the autocorrelation function $R_{\mathcal{N}}(\tau) = \text{E}(\mathcal{N}(t)\mathcal{N}(t-\tau))$, and we have the identity

$$\text{E}(\langle \mathcal{N} | \mathcal{F} \rangle \langle \mathcal{N} | \mathcal{F}' \rangle) = \langle \mathcal{F} | \mathcal{F}' \rangle. \quad (3)$$

The SNR $\rho_{\mathcal{F}}$ of the filtered data is then related to the true SNR ρ by

$$\rho_{\mathcal{F}}^2 = \frac{\langle \mathcal{S} | \mathcal{F} \rangle^2}{\langle \mathcal{F} | \mathcal{F} \rangle} \leq \langle \mathcal{S} | \mathcal{S} \rangle = \rho^2. \quad (4)$$

We now consider a generic bank of N GW templates $h_n(t)$, where the template labels n are drawn from the collection $\mathbf{N} := \{n \in \mathbb{Z}^+ | n \leq N\}$, and the templates have been normalised such that $\langle h_n | h_n \rangle = 1$ for all $n \in \mathbf{N}$. The inner products of the data (1) and the templates define N associated statistics

$$x_n := \langle \mathcal{X} | h_n \rangle, \quad (5)$$

which may be used for detection and identification in a simple grid search.

Our general method of compression is to reduce the number of statistic evaluations from N to M by considering conic combinations of the original templates. The template labels are grouped into M sets \mathbf{U}_m , where the set labels m are drawn from the collection $\mathbf{M} := \{m \in \mathbb{Z}^+ | m \leq M\}$, and the sets satisfy $\bigcup_{m \in \mathbf{M}} \mathbf{U}_m = \mathbf{N}$. These sets define M conic templates

$$H_m(t) := \sum_{n \in \mathbf{U}_m} h_n(t), \quad (6)$$

along with M associated statistics

$$X_m := \langle \mathcal{X} | H_m \rangle = \sum_{n \in \mathbf{U}_m} x_n. \quad (7)$$

Without any prior assumptions on the template bank, each template must be treated equally; this is done by ensuring (a) each combination is weighted equally, (b) each combination includes the same number of templates, and (c) each template is included in the same number of combinations. Definition (6) has been chosen to satisfy condition (a), while condition (b) is imposed by further requiring $\text{card}(\mathbf{U}_m) = \text{card}(\mathbf{U}_{m'})$ for all $m, m' \in \mathbf{M}$ (where the set cardinality $\text{card}(\mathbf{S})$ is the number of elements in the set \mathbf{S}). Condition (c) must be enforced separately in the construction of the sets. The second equality in Definition (7) relates the conic statistic evaluations to the original statistics (5), which are no longer evaluated at this coarser level.

To simplify analysis, we now assume the template bank is an orthogonal set such that

$$\langle h_n | h_{n'} \rangle = \delta_{nn'}, \quad (8)$$

where δ_{ij} is the Kronecker delta. We further assume the GW signal (if present) lies in the one-dimensional subspace spanned by a single template in Hilbert space, i.e.

$$\mathcal{S}(t) = Ah_1(t), \quad (9)$$

where $A > 0$ and the templates have been relabelled without loss of generality. It follows from (4) and (9) that $A = \rho$. The orthogonal and 1-D restrictions are not particularly realistic (especially when taken together), but facilitate the assessment and comparison of various compression schemes under idealised conditions. We address the lifting of these assumptions in Sec. IV.

In the presence of a GW signal, the expectation values and covariances of the normally distributed original statistics (5) are now given by

$$\text{E}(x_n) = A\delta_{1n}, \quad (10)$$

$$\text{cov}(x_n, x_{n'}) = \langle h_n | h_{n'} \rangle = \delta_{nn'}. \quad (11)$$

As the labelling of templates is itself a probabilistic process with discrete uniform distribution, the original statistic vector x has the multivariate Gaussian distribution $\mathcal{G}(\mu^{(i)}, \Sigma)$ (with $\mu_n^{(i)} = \mathbb{E}(x_n)$ and $\Sigma_{nn'} =$

$\text{cov}(x_n, x_{n'})$), but summed over the N possible assignments of $1 \in \mathbf{N}$ and renormalised accordingly. If the signal is absent, the distribution of x is simply $\mathcal{G}(0, \Sigma)$. Hence we have

$$p_1(x) \propto \frac{1}{N} \sum_{i=1}^N \exp\left(-\frac{1}{2}x^T \Sigma^{-1}x + \mu_{(i)}^T \Sigma^{-1}x - \frac{1}{2}\mu_{(i)}^T \Sigma^{-1}\mu_{(i)}\right), \quad (12)$$

$$p_0(x) \propto \exp\left(-\frac{1}{2}x^T \Sigma^{-1}x\right), \quad (13)$$

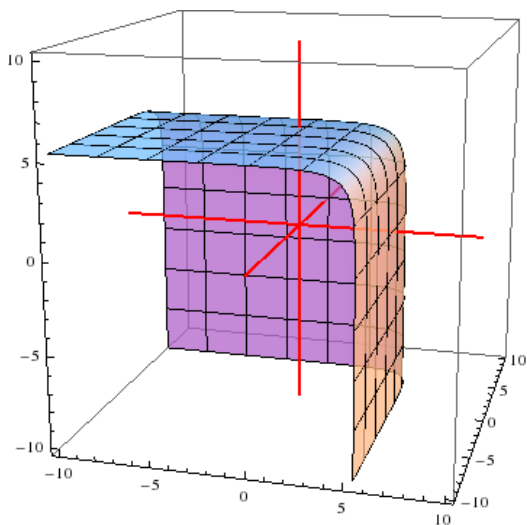


FIG. 1: Three-dimensional projection of an optimal detection surface for uncorrelated statistics, at a true SNR of 2.

where p_1 and p_0 are the probability density functions of x in the respective presence or absence of a GW signal.

An optimal detection region \mathcal{R} in Hilbert space maximises the detection rate $P_D = \int_{\mathcal{R}} p_1$ subject to a given false alarm rate $P_F = \int_{\mathcal{R}} p_0$; hence $p_1 = \lambda p_0$ on its boundary $\partial\mathcal{R}$ for some Lagrange multiplier λ . Using (10)–(13), we define the optimal detection statistic

$$x_{\text{opt}} := \frac{p_1(x)}{p_0(x)} = \frac{1}{N} \exp\left(-\frac{A^2}{2}\right) \sum_{n \in \mathbf{N}} \exp(Ax_n), \quad (14)$$

such that the optimal detection surfaces $\partial\mathcal{R}$ are precisely the level sets of x_{opt} parametrised by λ , and a detection is claimed if x_{opt} exceeds the threshold λ_T corresponding to some fixed value of P_F .

The optimal statistic (14) requires prior knowledge of the true SNR due to its dependence on A , and has to be approximated in practice. For sufficiently high SNR,

the optimal surfaces $x_{\text{opt}} = \lambda$ are well approximated by semi-infinite hypercubes in Hilbert space (see Fig. 1), i.e. the level sets of the standard grid-search detection statistic [18–20]

$$x_{\text{max}} = \max_{n \in \mathbf{N}} \{x_n\}. \quad (15)$$

Since the original statistics (5) are uncorrelated, the probability density functions of x_{max} in the presence or absence of a GW signal are obtainable explicitly. These are given respectively by

$$q_1(x_{\text{max}}) = F_0(x_{\text{max}})^{N-1} f_1(x_{\text{max}}) + (N-1)F_0(x_{\text{max}})^{N-2} F_1(x_{\text{max}}) f_0(x_{\text{max}}), \quad (16)$$

$$q_0(x_{\text{max}}) = NF_0(x_{\text{max}})^{N-1} f_0(x_{\text{max}}), \quad (17)$$

where $f_s(x_{\text{max}})$ is the probability density function for the Gaussian distribution $\mathcal{G}(sA, 1)$, and $F_s(x_{\text{max}})$ is the cumulative distribution function

$$F_s(x_{\text{max}}) = \int_{-\infty}^{x_{\text{max}}} f_s(u) du. \quad (18)$$

For our analysis of conic compression schemes, we also require the expectation values and covariances of the normally distributed conic statistics (7). From (7), (10) and (11), it follows in the presence of a GW signal that

$$\mathbb{E}(X_m) = \sum_{n \in \mathbf{U}_m} \mathbb{E}(x_n) = A \text{card}(\{1\} \cap \mathbf{U}_m), \quad (19)$$

$$\text{cov}(X_m, X_{m'}) = \sum_{n \in \mathbf{U}_m} \sum_{n' \in \mathbf{U}_{m'}} \text{cov}(x_n, x_{n'}) = \text{card}(\mathbf{U}_m \cap \mathbf{U}_{m'}), \quad (20)$$

where the cardinalities are determined by the choice of compression scheme. As before, the conic statistic vector X has the multivariate Gaussian distribution $\mathcal{G}(\mu^{(i)}, \Sigma)$

(now with $\mu_m^{(i)} = E(X_m)$ and $\Sigma_{mm'} = \text{cov}(X_m, X_{m'})$), but summed over the N possible assignments of $1 \in \mathbf{N}$ and renormalised accordingly. If the signal is absent, the distribution of X is again $\mathcal{G}(0, \Sigma)$. The probability density functions of X in the presence or absence of a GW signal are then given respectively by (12) and (13) with $x \equiv X$.

We now propose and investigate three general conic compression schemes in the remainder of Sec. II, before comparing their idealised performance and potential applicability in Sec. III.

A. Partition scheme

The simplest method of grouping the template labels n is to take the family of sets \mathbf{U}_m as a partition of \mathbf{N} , i.e. $\mathbf{U}_m \cap \mathbf{U}_{m'} = \emptyset$ for all distinct $m, m' \in \mathbf{M}$. Condition (c) in Sec. II is then automatically satisfied, while condition (b) defines the set cardinality $P = \text{card}(\mathbf{U}_m)$ for all $m \in \mathbf{M}$. It follows that $M = N/P$.

For the comparison of schemes in Sec. III, it is useful to introduce a common compression parameter $K \in \mathbb{Z}^+$ that determines the compression rate $\kappa := 1 - M/N$. This generates a sliding scale of groupings that ranges from no compression at $K = 1$ to maximal compression at some scheme-dependent value of K . We may clearly choose $K = P$ for the partition scheme, such that maximal compression is given by $K = N$. The minimal non-trivial compression is 50% at $K = 2$, while there are diminishing returns at large K since $\kappa(K)$ is concave-down.

From (19) and (20), we now have

$$E(X_m) = A\delta_{1m}, \quad (21)$$

$$\text{cov}(X_m, X_{m'}) = P\delta_{mm'}, \quad (22)$$

where the sets have been relabelled such that $1 \in \mathbf{U}_1$ without loss of generality. Again considering the N possible assignments of $1 \in \mathbf{N}$, the optimal detection statistic $X_{\text{opt}} := p_1(X)/p_0(X)$ follows from (12) and (13) (with $x \equiv X$) as

$$X_{\text{opt}} = \frac{1}{M} \exp\left(-\frac{A^2}{2P}\right) \sum_{m \in \mathbf{M}} \exp\left(\frac{A}{P}X_m\right). \quad (23)$$

Since the conic statistics for the partition scheme remain uncorrelated, the optimal surfaces $X_{\text{opt}} = \lambda$ resemble that in Fig. 1, and in lieu of (23) it is valid to consider the maximum-overlap detection statistic

$$X_{\text{max}} = \max_{m \in \mathbf{M}} \{X_m\}. \quad (24)$$

Receiver operating characteristic (ROC) curves of detection rate against false alarm rate for the optimal and maximum-overlap statistics are compared in Fig. 2 [28]. With increased compression, the performance of the

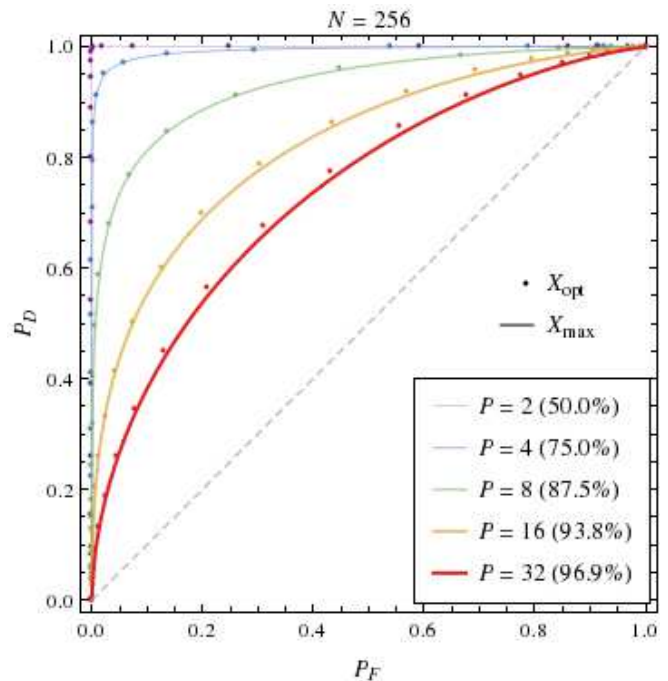


FIG. 2: ROC curves for the partition scheme's optimal and maximum-overlap detection statistics, at different values of set cardinality P (with compression rate κ in parentheses) for a 256-template bank and a true SNR of 10. In this figure (and all subsequent figures containing ROC curves), the dashed diagonal line indicates the worst possible performance, i.e. a random search for which the detection and false alarm rates are equal.

maximum-overlap statistic falls away slightly from that of the optimal statistic, due to the lowering of effective SNR A/\sqrt{P} in (23); nevertheless, (24) is a sound approximation as both sets of ROC curves show good overall agreement.

The trade-off between detection rate and compression for the partition scheme is dependent on the size of the template bank, and in general grows poorer as N increases. ROC curves (using the maximum-overlap statistic (24)) for a 6561-template bank and a true SNR of 10 are shown in Fig. 3. By comparison with Fig. 2 for a 256-template bank and the same SNR, it may be seen that a similar compression rate ($P = 32$ in Fig. 2 and $P = 27$ in Fig. 3) retains better performance for the smaller template bank. This is expected since we have assumed the GW signal lies in the span of the template bank, which is a stronger assumption to begin with in the case of smaller N .

For the partition scheme to admit a useful (i.e. populated) sliding scale of compression rates, the template bank might need to be trimmed or padded such that N has as many divisors as possible (e.g. N is a power of 2 or 3). Fixing the false alarm rate and choosing either a desired detection rate or a compression rate then allows advance determination of the conic templates (6) and the

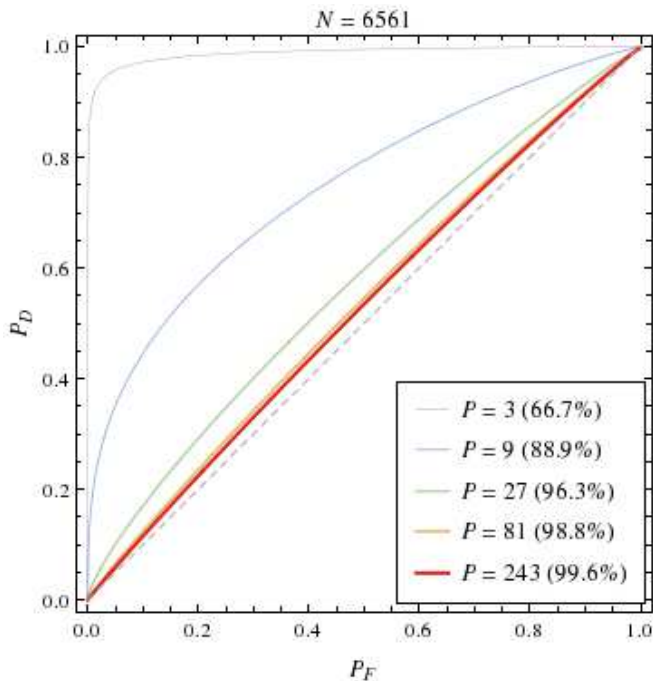


FIG. 3: ROC curves for the partition scheme's maximum-overlap detection statistic, at different values of set cardinality P (with compression rate κ in parentheses) for a 6561-template bank and a true SNR of 10.

threshold λ_T , which is the value of λ corresponding to the fixed false alarm rate. The algorithm for GW detection follows as: (i) evaluate the conic statistics (7); (ii) claim a detection if $X_{\max} > \lambda_T$. Threshold and detection SNRs may be defined respectively as

$$\rho_T := \frac{\lambda_T}{\sqrt{\text{var}(X_{\max})}} \approx \frac{\lambda_T}{\sqrt{P}}, \quad (25)$$

$$\rho_D := \frac{X_{\max}}{\sqrt{\text{var}(X_{\max})}} \approx \frac{X_{\max}}{\sqrt{P}}, \quad (26)$$

with the approximations becoming equalities in the limit of infinite true SNR.

An extension of the detection algorithm is required for the purposes of GW identification, since the simple coarse-graining of partition compression does not distinguish between template labels in the same set. The signal is most likely to be associated with the largest conic statistic evaluation $X_{(1)}$, so the best candidate template may be obtained by further evaluating all the original statistics x_n contributing to $X_{(1)}$ and identifying the largest. This finer level of evaluations increases the computational cost from M to $M + P$.

For better identification accuracy at lower SNR, we may widen our search to the i largest X_m instead, at an added computational cost of iP . The standard algorithms I_i for GW identification follow (after detection)

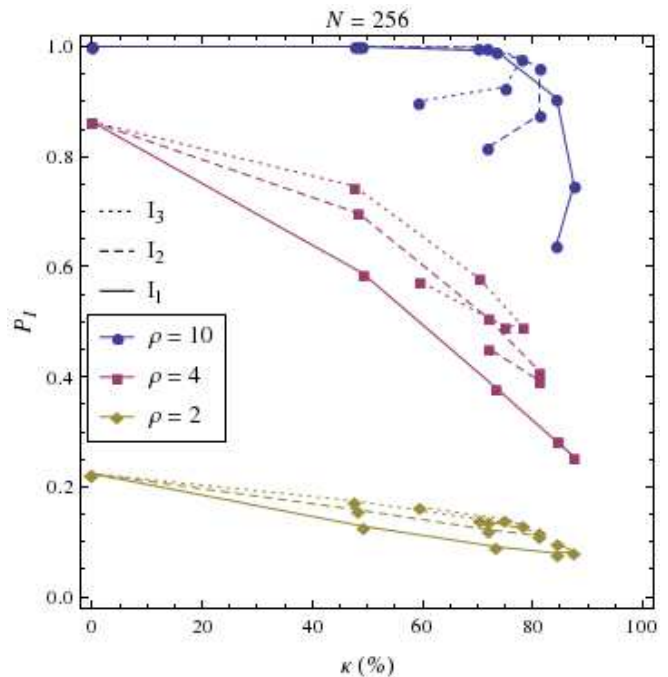


FIG. 4: Plots of accurate identification rate P_I against compression rate κ for the partition scheme's standard identification algorithms, at different values of true SNR ρ for a 256-template bank.

as: (iii) evaluate the original statistics (5) for all $n \in \mathbf{V}_i$, where

$$\mathbf{V}_i = \bigcup_{j=1}^i \mathbf{U}_{(j)}, \quad (27)$$

with $\mathbf{U}_{(j)}$ corresponding to the j -th largest conic statistic evaluation; (iv) identify $\max_{n \in \mathbf{V}_i} \{x_n\}$.

Other identification algorithms may also be considered. One such alternative is obtained by defining a further partition of \mathbf{V}_i into two sets and evaluating the associated conic statistics, then identifying the set \mathbf{V}'_i corresponding to the larger statistic evaluation and repeating the process with $\mathbf{V}_i \equiv \mathbf{V}'_i$ until $\text{card}(\mathbf{V}'_i) = 1$. This method might be useful for large values of P ; it yields a smaller added computational cost of $2 \log_2 iP$, but incurs a penalty to identification accuracy since the early iterations still involve coarse-grained searches.

Fig. 4 shows a comparison of the standard identification algorithms I_1 – I_3 at different values of true SNR, with plots of accurate identification rate P_I (given a true detection) against compression rate κ (taking into account the fine-grained search) for $N = 256$ and $1 \leq P \leq 32$. In general, the absolute fall-off in identification accuracy is least severe for high-SNR signals with small P , but also for low-SNR signals where the accuracy is poor to begin with. For small values of P , which are more important for practical purposes, I_3 offers potentially significant improvement in accuracy over $I_{i < 3}$ at the cost of a slight loss

in compression. Large values of P give suboptimal accuracy for their compression at high SNR (i.e. the $\rho = 10$ plots in Fig. 4 curve back under themselves), but actually provide marginally better performance at low SNR (the $\rho = 2$ plots curve back over themselves).

B. Symmetric base scheme

Without an additional fine-grained search, partition compression is lossy in the sense that the GW signal is not automatically identified in the limit of zero noise. A recently proposed conic compression scheme introduces a lossless method of compression, by representing each template label n in binary and assigning it to the set \mathbf{U}_m if its m -th digit is 1 [17]. This binary scheme features the largest possible lossless compression ($M = \log_2 N$) and an automatic identification of the GW signal; however, it suffers from an unequal treatment of templates (i.e. it violates conditions (b) and (c) in Sec. II) and hence an arbitrary level of performance that depends on the initial assignment of template labels. Furthermore, the restriction to maximum compression is impractical for all but the highest-SNR GW signals.

We propose a compression scheme modelled on the binary labelling method, but symmetrised (for equal treatment of templates) and generalised to a sliding scale of base representations (for tunable compression). The template labels n are represented modulo N in base B , and each set $\mathbf{U}_m \equiv \mathbf{U}_{k,b}$ is constructed by collecting all the labels whose k -th digit is b (this includes $b = 0$, and gives a symmetric version of the binary scheme [17] when $B = 2$). For conditions (b) and (c) in Sec. II to be satisfied, we require $\log_B N \in \mathbb{Z}^+$; it follows that $M = B \log_B N$.

The compression parameter is chosen as $K = \log_B N$, such that maximal compression is given by $K = \log_3 N \approx \ln N$ (base-2 compression is slightly suboptimal with symmetrisation). In contrast to the partition scheme, compression for the symmetric base scheme is dependent on the size of the template bank; the minimal nontrivial compression for $N = 10^2$ is nearly 80% at $K = 2$ (base- \sqrt{N} compression), and over 95% for $N = 10^4$. The only practical setting for larger template banks is $K = 2$, due to the rapidly diminishing returns at greater values of K .

From (19) and (20), we have

$$\mathbb{E}(X_m) = A\delta_{0b}, \quad (28)$$

$$\text{cov}(X_m, X_{m'}) = B^{K-2}(B\delta_{kk'}\delta_{bb'} - \delta_{kk'} + 1), \quad (29)$$

where $m = B(k-1) + b + 1$, and the templates have been relabelled such that $\mathcal{S}(t) = Ah_N(t)$ without loss of generality [29]. Considering the N possible assignments of $N \in \mathbb{N}$, the optimal detection statistic follows from

(12) and (13) as

$$X_{\text{opt}} = \frac{1}{N} \exp\left(-\frac{\beta K A^2}{2} + (\beta - \alpha)A \text{tr}(X)\right) \times \prod_{k=1}^K \sum_{b=0}^{B-1} \exp(\alpha A X_{k,b}), \quad (30)$$

$$\alpha = \frac{B}{N}, \quad \beta = \frac{M - K + 1}{NK}, \quad (31)$$

where $\text{tr}(X) := \sum_{m \in \mathbf{M}} X_m$.

The higher compression rates provided by the symmetric base scheme result from the non-empty intersections among the sets $\mathbf{U}_{k,b}$ with different values of k . As seen in (29), these also lead to correlations among the conic statistics $X_{k,b}$. The optimal detection surfaces given by $X_{\text{opt}} = \lambda$ differ significantly from that depicted in Fig. 1; their projections onto the correlated subspaces are now compact hyperboloids, and no longer approach the semi-infinite hypercubes of the maximum-overlap detection statistic at high SNR (see Fig. 5).

Without a simple approximation for the optimal detection statistic, the most feasible option is to use (30) itself with an estimate A of the true SNR. ROC curves for the estimated statistic $X_{\text{opt}}^{A=\epsilon\rho}$ with $\epsilon \in \{1/2, 2\}$ are compared against those for the optimal and maximum-overlap statistics in Fig. 6. Not much detection sensitivity (for a fixed false alarm rate) is lost if the true SNR can be estimated to within a factor of two, while usage of the maximum-overlap statistic now incurs a noticeable drop in performance as expected.

For larger template banks, even the minimal nontrivial compression might be excessive if the true SNR is not sufficiently high. Fig. 7 shows ROC curves (using the optimal statistic (30)) for a 6561-template bank and a true SNR of 10; both the compression and the performance lost at $B = 81$ ($K = 2$) are substantial, which limits the usefulness of the symmetric base scheme at the given values of N and ρ .

The restriction of N , B and K to integer values also results in more sparsely populated sliding scales than those admitted by the partition scheme. There are three possible compression rates for $N = 6561$, and two for $N = 256$ (base-2 compression is suboptimal compared to $B = 4$); most other values of N will admit only one or none. Notwithstanding the lack of tunability, a feasible strategy is to trim or pad the template bank such that N is a perfect square or cube, since the smallest values of K are the most important anyway (especially for large N). The GW detection algorithm then follows as given in Sec. II A, with some estimated detection statistic $X_{\text{opt}}^{A=\epsilon\rho}$ in place of X_{max} .

One key feature of the symmetric base scheme and other lossless methods of compression is automatic identification of the GW signal (upon detection). In this case, the label of the identified template in base- B representation is given digit-wise by the largest conic statistic eval-

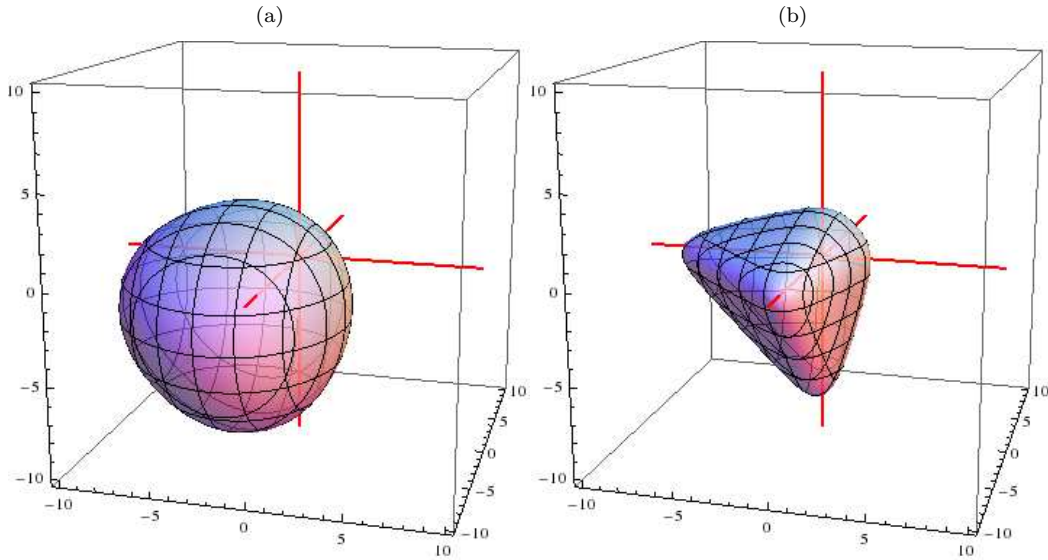


FIG. 5: Three-dimensional projection of an optimal detection surface for the symmetric base scheme's correlated statistics, at true SNRs of (a) 10 and (b) 100.

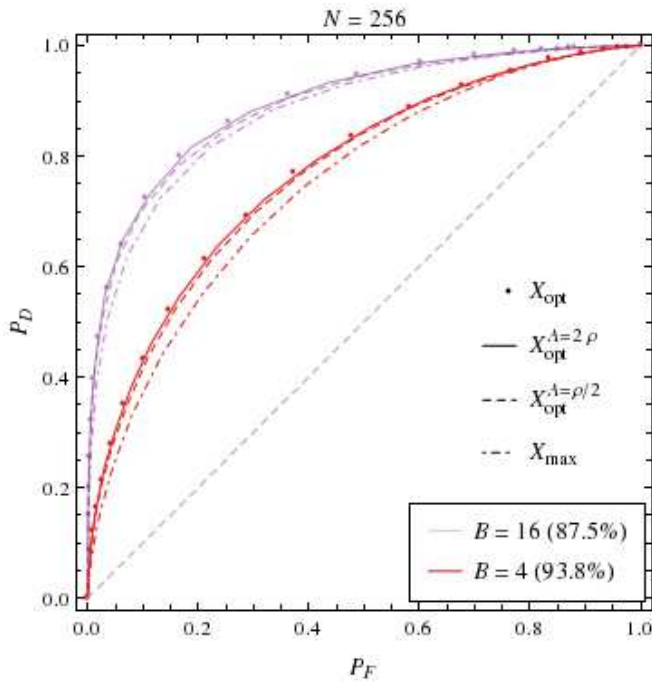


FIG. 6: ROC curves for the symmetric base scheme's optimal, maximum-overlap and estimated detection statistics, at different values of base B (with compression rate κ in parentheses) for a 256-template bank and a true SNR of 10.

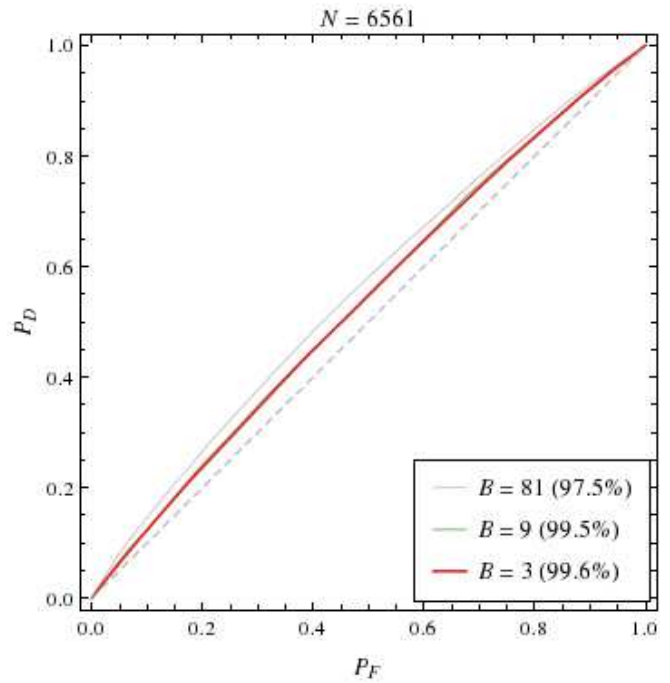


FIG. 7: ROC curves for the symmetric base scheme's optimal detection statistic, at different values of base B (with compression rate κ in parentheses) for a 6561-template bank and a true SNR of 10. The curves for $B = 3$ and $B = 9$ are almost indistinguishable.

uation $X_{k,(1)} := \max_b \{X_{k,b}\}$ for each value of k . However, as each digit k is identified individually, the overall identification accuracy falls off severely with increasing K (i.e. the total number of digits).

A possible modification for better accuracy is to consider the $i + 1$ largest $X_{k,b}$ for each k and perform an additional fine-grained search over the $(i + 1)^K$ templates, which increases the computational cost accordingly. The

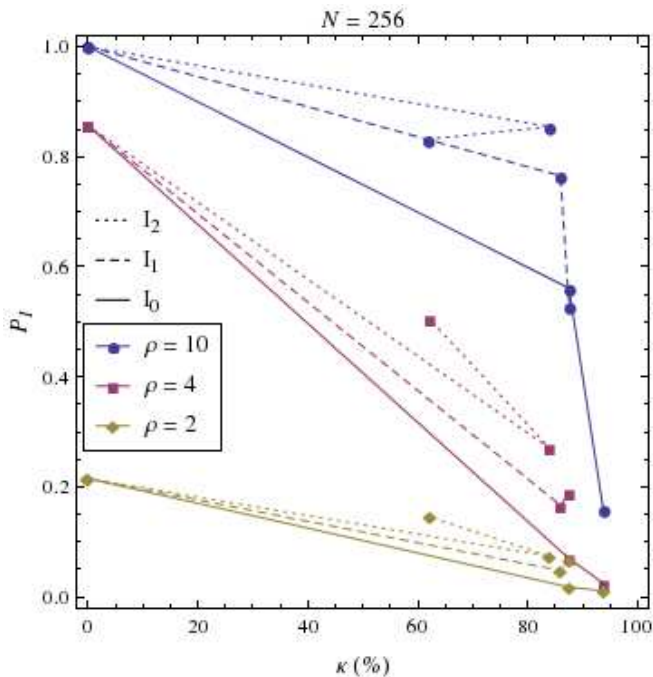


FIG. 8: Plots of accurate identification rate P_I against compression rate κ for the symmetric base scheme's standard identification algorithms, at different values of true SNR ρ for a 256-template bank.

standard GW identification algorithms I_i follow (after detection) as: (iii) evaluate the original statistics (5) for all $n \in \mathbf{V}_i$, where

$$\mathbf{V}_i = \bigcap_{k=1}^K \bigcup_{j=1}^{i+1} \mathbf{U}_{k,(j)}, \quad (32)$$

with $\mathbf{U}_{k,(j)}$ corresponding to the j -th largest conic statistic evaluation for each k ; (iv) identify $\max_{n \in \mathbf{V}_i} \{x_n\}$. Automatic identification is recovered for $i = 0$, where steps (iii) and (iv) become unnecessary as $\text{card}(\mathbf{V}_0) = 1$.

For large values of K (small values of B), the standard identification algorithms might still suffer from poor accuracy. One alternative algorithm is obtained by defining some threshold X_T and considering all conic statistic evaluations $X_{k,b} \geq X_T$, then performing the additional fine-grained search over all the corresponding templates. Such a threshold may be set prior to data-taking; if $X_{k,(1)} < X_T$ for some value of k , the k -th digit of the number is unconstrained and templates corresponding to all possible choices of that digit are considered. Alternatively, X_T may be based on the data by setting $X_T = f \min_k \{X_{k,(1)}\}$ for some fixed fraction f , which ensures that at least one possible value is identified for each digit. Both approaches will in general yield increased accuracy, but they offer less control over the number of conic statistic evaluations considered and hence the overall computational cost.

Fig. 8 shows a comparison of the standard identifica-

tion algorithms I_0 – I_2 at different values of true SNR, for $N = 256$ and $256 \geq B \geq 4$. For the minimal nontrivial compression ($B = 16$), the fall-off in accuracy for automatic identification is well mitigated by switching to $I_{i>0}$. This is not necessarily the case for $B = 4$, where accuracy is gained at the cost of greater compression loss; the accuracy–compression trade-off actually becomes suboptimal at high SNR (i.e. the $\rho = 10$ plot for I_2 in Fig. 8 curves back under itself).

C. Binomial coefficient scheme

The symmetric base labelling method is not the only construction of the sets \mathbf{U}_m that preserves both lossless compression (automatic identification) and equal treatment of templates (conditions (b) and (c) in Sec. II). In general, we may represent any assignment of N templates to M sets with a collection of N M -digit binary labels, where the m -th digit of each label is 1 if it appears in \mathbf{U}_m and 0 otherwise. Condition (c) implies that each label must appear in exactly R sets, and hence contain exactly R 1's. In addition, condition (b) defines the set cardinality $C = \text{card}(\mathbf{U}_m)$ for all $m \in \mathbf{M}$, which yields the constraint $NR = MC$ (each of the N labels appears exactly R times across all sets, while each of the M sets contains exactly C labels). For some given integers $N \geq M \geq R$, this constraint is equivalent to the existence of

$$C = \frac{NR}{M} \in \mathbb{Z}^+, \quad (33)$$

which is both a necessary and sufficient condition for such a set construction to be possible [21].

We now require that the conic statistics (7) are correlated symmetrically, as seen in the partition scheme (but not the symmetric base scheme). This additional condition implies that the intersection of each pair of sets has fixed cardinality I , i.e. $\text{card}(\mathbf{U}_m \cap \mathbf{U}_{m'}) = I$ for all distinct $m, m' \in \mathbf{M}$. Considering the family of all such intersections then yields the constraint $NR(R-1) = M(M-1)I$ (each of the N labels appears exactly ${}^R C_2$ times across all intersections, while each of the ${}^M C_2$ intersections contains exactly I labels). For some given integers $N \geq M \geq R$ and C satisfying (33), this constraint is equivalent to the existence of

$$I = \frac{NR(R-1)}{M(M-1)} = \frac{C(R-1)}{M-1} \in \mathbb{Z}^+, \quad (34)$$

which is a necessary (but not in general sufficient) condition for such a set construction to be possible.

If the conditions (33) and (34) are satisfied, the problem of constructing a family of sets \mathbf{U}_m may be regarded geometrically as the problem of constructing a collection of N distinct points (representing template labels) and M distinct lines (representing sets) with the following properties: (i) each point lies on exactly R lines; (ii) each

line passes through exactly C points; (iii) any two lines intersect at exactly I points; (iv) any two points lie on at most $R - 1$ lines. The final property is the automatic identification condition, i.e. no two labels are assigned to exactly the same subfamily of sets.

The feasibility of carrying out such a construction (or finding additional conditions on N , M and R that ensure it is possible) is a difficult and unsolved problem in combinatorics. One special case that has been studied in detail is $R = C$ and $I = 1$. This implies that $N = M = R^2 - R + 1$, and that any two points must lie on exactly one line. Under these circumstances, the four geometrical properties define a finite projective plane of order $R - 1$ [21]. It is known that finite projective planes exist with prime orders [21], but there is no finite projective plane of order 6 [22] or 10 [23], while the existence (or otherwise) of an order-12 finite projective plane remains an open question.

The special case of finite projective planes is uninteresting from a compression-scheme point of view, as it has $N = M$ and hence achieves no compression. However, it strongly indicates that the conditions (33) and (34) are not sufficient to ensure the existence of a set construction with the four required properties. Nonetheless, valid set constructions have been found for small values of N , M and R ; for example, $(N, M, R) = (10, 6, 3)$ yields $C = 5$, $I = 2$, and the set construction

$$\begin{aligned} \mathbf{U}_1 &= \{1, 2, 3, 4, 5\}, \\ \mathbf{U}_2 &= \{1, 2, 6, 7, 8\}, \\ \mathbf{U}_3 &= \{1, 3, 6, 9, 10\}, \\ \mathbf{U}_4 &= \{2, 5, 8, 9, 10\}, \\ \mathbf{U}_5 &= \{3, 4, 7, 8, 10\}, \\ \mathbf{U}_6 &= \{4, 5, 6, 7, 9\}. \end{aligned} \quad (35)$$

Additional solutions for $(N, M, R) = (12, 9, 3)$ and $(N, M, R) = (14, 7, 3)$ also exist. No counterexamples (i.e. values of (N, M, R) satisfying (33) and (34) but admitting no set construction) have been found for $N > M$, although we have not conducted an exhaustive search.

The set construction method described in this section thus far is quite general, and might potentially admit more compression rates than the symmetric base scheme for each value of N . Given the difficulties in actually constructing the sets, however, we restrict our focus to a special case that may be treated in greater detail. This is the case of ‘‘maximal representation’’ for fixed M and R , i.e. every M -digit binary number with exactly R 1’s represents a distinct template label, such that $N = {}^M C_R$. The set cardinality then equals the number of $(M - 1)$ -digit binary numbers with exactly $(R - 1)$ 1’s, while the intersection cardinality of each pair of sets equals the number of $(M - 2)$ -digit binary numbers with exactly $(R - 2)$ 1’s. Hence for all distinct $m, m' \in \mathbf{M}$, we have

$$C = {}^{M-1}C_{R-1}, \quad I = {}^{M-2}C_{R-2}, \quad (36)$$

such that the conditions (33) and (34) are satisfied. We refer to this as the binomial coefficient scheme, for ob-

vious reasons. The usual ordering of the binary numbers gives a natural map onto the original label collection $\mathbf{N} = \{n \in \mathbb{Z}^+ | n \leq N\}$, although the inverse map is analytically nontrivial (but straightforward in practice).

As the binomial coefficient scheme shares many similarities with the symmetric base scheme, we only highlight its key features in this section. The compression parameter is chosen as $K = R$, such that maximal compression is given by $K = \text{cbc}^{-1}(N)/2$ (where $\text{cbc}(M) := \Gamma(M + 1)/\Gamma(M/2 + 1)^2$ is the continuous extension of the central binomial coefficient ${}^M C_{M/2}$). Compression rates again depend on the size of the template bank; at small values of K , they are only slightly higher than those of the symmetric base scheme.

From (19) and (20), we have

$$E(X_m) = A \sum_{r=1}^R \delta_{rm}, \quad (37)$$

$$\text{cov}(X_m, X_{m'}) = {}^{M-2}C_{R-2} \left(\frac{M-R}{R-1} \delta_{mm'} + 1 \right), \quad (38)$$

where the sets have been relabelled such that $1 \in \mathbf{U}_r$ for $1 \leq r \leq R$ without loss of generality. Considering the N possible assignments of $1 \in \mathbf{N}$, the optimal detection statistic follows from (12) and (13) as

$$\begin{aligned} X_{\text{opt}} &= \frac{1}{N} \exp \left(-\frac{\beta K A^2}{2} + (\beta - \alpha) A \text{tr}(X) \right) \\ &\quad \times \sum_{i=1}^N \exp \left(\alpha A \sum_{r \in \mathbf{R}_i} X_r \right), \end{aligned} \quad (39)$$

$$\alpha = \frac{1}{{}^{M-1}C_{R-1}}, \quad \beta = \frac{1}{{}^{M-2}C_{R-1}}, \quad (40)$$

where the sets \mathbf{R}_i are the N distinct R -combinations of \mathbf{M} .

All the conic statistics X_m are correlated symmetrically, as seen in (38). Upon projection onto any three-dimensional subspace, the optimal detection surfaces given by $X_{\text{opt}} = \lambda$ resemble those in Fig. 5 at both low and high SNR. It follows that the maximum-overlap detection statistic is again an inadequate approximation to the optimal statistic, and we are compelled to use (39) itself (assuming an accurate estimate of true SNR). We do not include ROC curves for the binomial coefficient scheme here, as they are very similar to those in Figs 6 and 7; for a true SNR of 10, they show a significant drop in performance when the size of the template bank is increased from $N \approx 256$ to $N \approx 6561$.

A direct comparison of the base and binomial schemes is difficult, since their performance depends on the size of the template bank and there are few suitable values of N that are exactly valid for both schemes. Lack of tunability is also more of an issue for the binomial scheme:

the only values of N that admit more than one nontrivial compression rate might be the Singmaster numbers (which admit two as they appear six times in Pascal's triangle), and it is not known whether any number admits more than two (apart from $3003 = {}^{78}C_2 = {}^{15}C_5 = {}^{14}C_6$) [24, 25]. The problem may be overcome by considering the more general compression scheme described at the start of this section. Given the complexity of set construction in that case, such a generalisation is beyond the scope of the current paper, but might be investigated for specific template banks in the future.

The GW detection algorithm for the binomial coefficient scheme is as given in Sec. II A, with some estimated detection statistic $X_{\text{opt}}^{A=\epsilon\rho}$ in place of X_{max} . Automatic identification is available as well, with the label of the identified template given uniquely by the R largest conic statistic evaluations. For higher accurate identification rates, a possible alternative is to consider the $R+i$ largest X_m and perform an additional fine-grained search over the ${}^{R+i}C_R$ templates. The standard GW identification algorithms I_i follow (after detection) as: (iii) evaluate the original statistics (5) for all $n \in \mathbf{V}_i$, where

$$\mathbf{V}_i = \bigcup_{k=1}^{R+i} \bigcap_{j \in \mathbf{J}_k} \mathbf{U}_{(j)}, \quad (41)$$

with $\mathbf{U}_{(j)}$ corresponding to the j -th largest conic statistic evaluation and the sets \mathbf{J}_k given by the ${}^{R+i}C_R$ distinct R -combinations of $\{j \in \mathbb{Z}^+ | j \leq R+i\}$; (iv) identify $\max_{n \in \mathbf{V}_i} \{x_n\}$. Automatic identification is recovered for $i=0$, where steps (iii) and (iv) become unnecessary as $\text{card}(\mathbf{V}_0) = 1$.

We note that another possible scheme would be a ‘‘direct sum’’ of the partition scheme and either the symmetric base or binomial coefficient scheme. The collection of template labels is first partitioned into subcollections, each of which is further decomposed into smaller sets via one of the correlated schemes; these sets may also be recombined across the initial partition for increased compression. We do not consider this further here, but such an approach would overcome some of the difficulties associated with the restricted values of N for the base and binomial schemes.

III. PERFORMANCE COMPARISON

In this section, we compare the performance of the uncorrelated partition scheme and its two correlated alternatives across three areas: template bank compression, GW detection and GW identification.

Log-log plots of M against N for various conic compression schemes are shown in Fig. 9, where the maximum lossless compression provided by the binary scheme [17] has also been included for reference. As alluded to in Sec. II, the partition scheme has the largest range of compression rates, both in terms of compression bounds (plot

area) and admitted rates (discrete density, not shown). The two correlated schemes cover similar areas at lower densities in Fig. 9, with the binomial coefficient scheme offering slightly greater compression.

Detection performance for each compression setting of a given scheme may be measured by detection sensitivity at a fixed false alarm rate (which is simply read off the corresponding ROC curve), or by a summary statistic that captures most of the information contained in an ROC curve (e.g. the area A_{ROC} under the curve). Since an ROC curve always lies above the no-discrimination line $P_D = P_F$, we define the discrimination $D := 2A_{\text{ROC}} - 1$ as a measure of how well the corresponding detection statistic discriminates between true and false positives.

Fig. 10 (a) shows plots of discrimination against compression for the three proposed schemes at different values of true SNR, with $N \approx 256$. We use the maximum-overlap detection statistic in lieu of the optimal statistic for the partition scheme, and are compelled to choose $N = 210$ for the binomial coefficient scheme; at low SNR, these choices slightly degrade the performance of the former and boost that of the latter. The three schemes have comparable performance at low SNR, but the partition scheme clearly outpaces its correlated alternatives as SNR increases. Detection performance for the partition scheme also scales more favourably with N . For $N \approx 6561$, the SNR required for $D > 0.5$ at the minimal nontrivial compression is $5 < \rho < 10$ for the partition scheme and $20 < \rho < 25$ for the correlated schemes.

To compare identification performance, we again consider plots of accurate identification rate against compression, but only for the fastest standard algorithms of each scheme (i.e. I_1 for the partition scheme, and automatic identification I_0 for the correlated schemes). As seen in Fig. 10 (b), the usefulness of lossless compression and automatic identification is limited in the presence of noise; the addition of a simple fine-grained search to the partition scheme is enough to yield significantly higher identification accuracy even at marginally lower compression.

In summary, the partition scheme offers better overall performance than its correlated alternatives at the same level of compression. This is expected for GW detection since the introduced correlations among the conic statistics increase the log determinant of their covariance matrix, reducing detection sensitivity and discriminatory power; furthermore, the potential benefits of lossless compression for GW identification turn out to be nullified by the effects of noise. Hence any correlated schemes will be practical for GW grid searches only if both the computational cost and the expected SNR are extremely high. The partition scheme is more promising as it is easy to implement, scales well with N and admits a relatively populated sliding scale of compression rates. It also lends itself to the customisation of partitions, which we discuss in the following section.

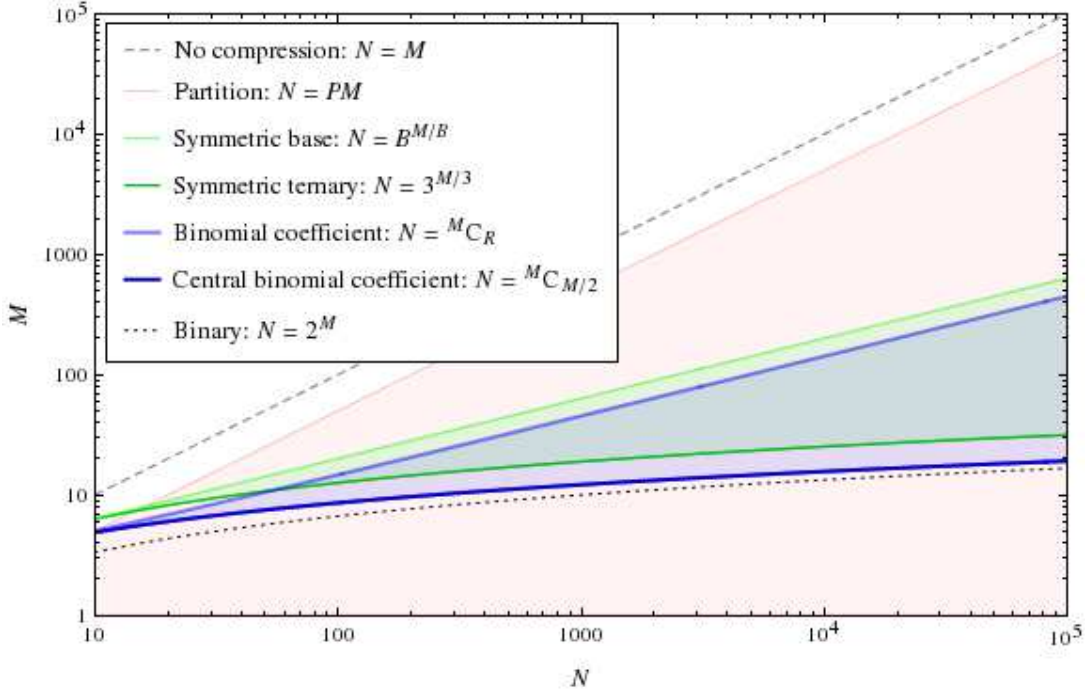


FIG. 9: Log-log plots of M against N for various compression schemes. For each tunable scheme, the corresponding shaded region indicates the range of possible compression rates (with the trivial compression setting $K = 1$ excluded). Not every point in this region is realisable in practice, as discussed in the text.

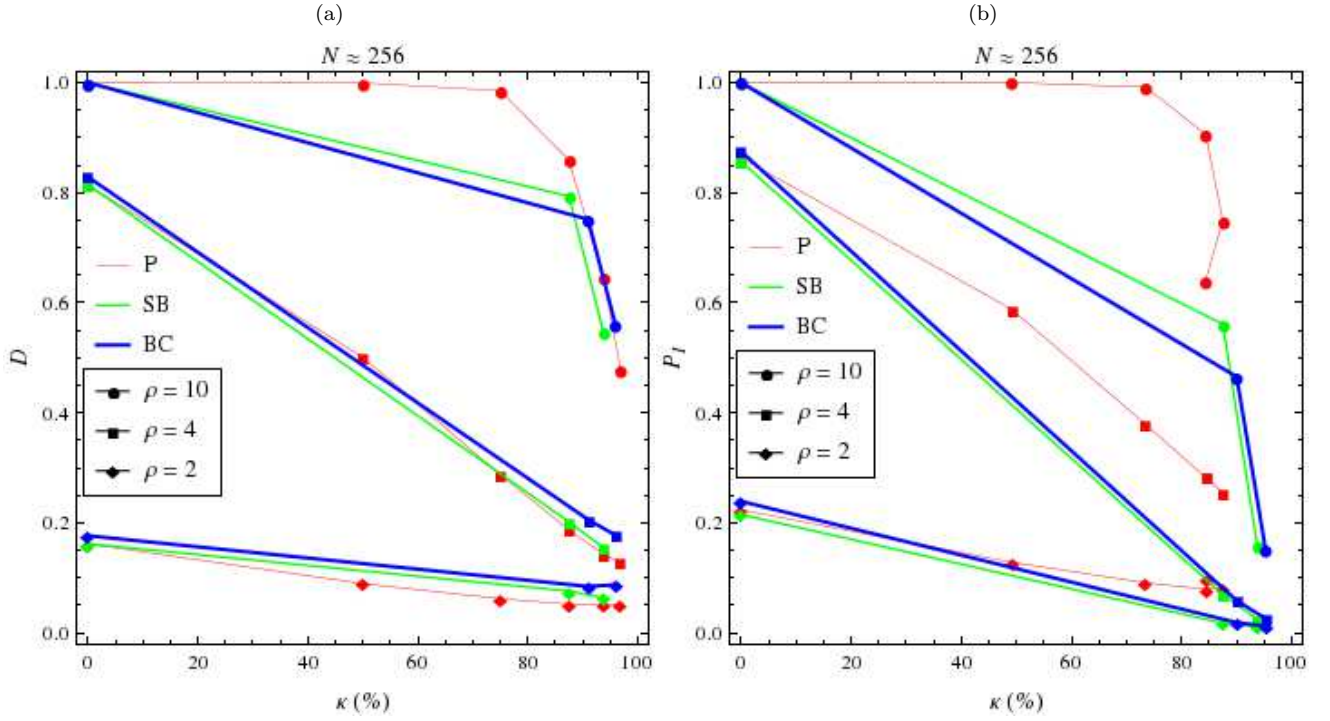


FIG. 10: Plots of (a) discrimination D and (b) accurate identification rate P_I against compression rate κ for the partition, symmetric base and binomial coefficient schemes, at different values of true SNR ρ for a ≈ 256 -template bank.

IV. ORTHOGONALITY AND SUBSPACES

The conic compression schemes proposed in Sec. II are fully general, in the sense that no prior assumptions about the template bank are made apart from (8) and (9). These orthogonal and 1-D conditions are highly idealised when taken together, but may be imposed individually (at the expense of the other) through the respective usage of an orthogonalised or densely sampled template bank. In this section, we discuss the lifting of each assumption for the partition scheme, and the resultant effects on both detection sensitivity and identification accuracy.

We first consider a sufficiently dense bank of correlated (non-orthogonal) templates, such that the GW signal still lies in the 1-D subspace spanned by a single template in Hilbert space. The nonzero covariances of the original statistics (5) alter the covariances of the conic statistics (7) accordingly, via the first equality in (20). With

$$\langle h_n | h_{n+\Delta n} \rangle \approx 2 \int_0^1 \sin(2\pi f_{\min} t) \sin(2\pi(f_{\min} + |\Delta n| \delta f)t) dt, \quad (43)$$

where we have normalised to $T = 1$ such that f is given in waveform cycles per observation time. This sinc-like function of $\Delta n \in \mathbb{Z}$ yields a band covariance matrix for x_n ; we set $N = 256$, and choose the frequency bounds such that $\text{cov}(x_n, x_{n\pm 1}) \approx 0.97$ [26, 27].

In contrast to the orthogonal case, the choice of partition generally affects the performance of the partition scheme for non-orthogonal templates. We consider three choices for the template bank with overlaps given by (43): an unsorted partition with $\mathbf{U}_m = \{n \in \mathbb{Z}^+ | (m-1)P < n \leq mP\}$, a randomised partition, and a more optimised (but not necessarily optimal) partition with $\mathbf{U}_m = \{n \in \mathbb{Z}^+ | n \equiv m \pmod{M}\}$. The standard detection and identification algorithms outlined in Sec. II A may then be applied for each.

Fig. 11 shows plots of discrimination (using X_{\max}) and accurate identification rate (using \mathbf{I}_1) against compression for the three choices of partition. The overall performance is seen to be highly partition-dependent, with the optimised partition showing significant improvement over its unsorted counterpart at all considered values of true SNR. An uptick in performance is also observed for the optimised partition at $P = 32$, which coincides with a separation between labels (in each \mathbf{U}_m) that exceeds the cycle width of (43).

A feasible strategy to optimise the partition scheme for non-orthogonal templates is to “spread” the generalised variance of the original statistics by decreasing the variance of each conic statistic, which in turn decreases the upper bound on the log determinant of the conic covariance matrix given by Hadamard’s inequality for positive-

any partition of \mathbf{N} in Sec. II A defining a partition of the (sorted) original covariance matrix $\Sigma_{nn'}$ into $P \times P$ blocks, the second term in (20) is precisely the sum of entries in each block, which provides a simple method of obtaining the conic covariance matrix $\Sigma_{mm'}$.

In our idealised (but physically motivated) investigation of the partition scheme for non-orthogonal templates, we use a frequency-parametrised bank of sinusoidal waveforms $h = \sin(2\pi ft)$ with finite observation time T . Assuming white noise for simplicity, the inner product (2) may be written as

$$\langle \mathcal{X} | \mathcal{F} \rangle \propto \int_0^T \mathcal{X}(t) \mathcal{F}(t) dt. \quad (42)$$

For an N -template bank with $f_{\min} \leq f \leq f_{\max}$ and $\delta f := (f_{\max} - f_{\min}) / (N - 1) \ll f_{\min}$, the overlaps are then given by

definite matrices. While a lowered upper bound does not guarantee a decrease in the quantity itself, this strategy should push the scheme in the direction of decreasing log determinant. The spreading of generalised variance is generally achieved by ensuring that labels of highly correlated templates are not assigned to the same \mathbf{U}_m , as seen from the first equality in (20). Another possibility for further customisation would be to allow weighted combinations of varying length in (6) (i.e. to lift conditions (a) and/or (b) in Sec. II), which might be used to incorporate any prior information on the template bank or assumptions on the GW signal.

We now consider a bank of uncorrelated templates obtained through some orthogonalisation procedure on the template bank given above, such that the GW signal now lies generally in the N -dimensional Hilbert space spanned by the orthogonal set. Since the overlaps in (43) are highly localised, however, the signal is effectively restricted to a low-dimensional subspace. For simplicity, we assume it lies exactly between two templates in a 2-D subspace, i.e.

$$\mathcal{S}(t) = A(h_1(t) + h_2(t)), \quad (44)$$

where the templates have been relabelled without loss of generality and $A = \rho / \sqrt{2}$ from (4). Hence the expectation values of the original and conic statistics become

$$\mathbf{E}(x_n) = A(\delta_{1n} + \delta_{2n}), \quad (45)$$

$$\mathbf{E}(X_m) = A \text{card}(\{1, 2\} \cap \mathbf{U}_m), \quad (46)$$

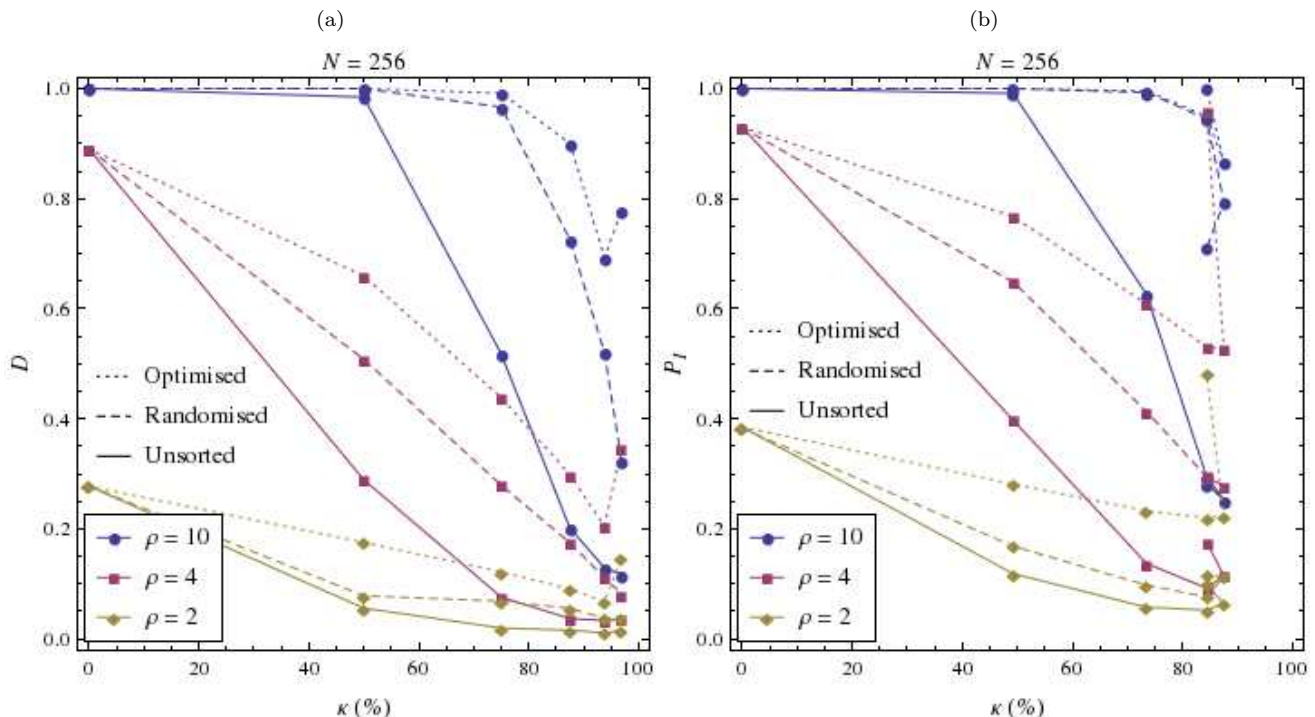


FIG. 11: Plots of (a) discrimination D and (b) accurate identification rate P_I against compression rate κ for the sorted partition schemes, at different values of true SNR ρ for a non-orthogonal 256-template bank.

while their covariances remain as (11) and (20) respectively.

Although it is not possible to pre-optimize the choice of partition for orthogonal templates, the performance of the partition scheme in the presence of a 2-D GW signal (44) falls into two partition-dependent cases. At small values of P , it is more likely that the labels $1 \in \mathbf{U}_m$ and $2 \in \mathbf{U}_{m'}$ are assigned to different sets ($m \neq m'$); as P increases, so does the probability that they are assigned to the same set ($m = m'$), which improves performance (e.g. the effective SNR for detection purposes is raised by a factor of $\sqrt{2}$).

The standard detection algorithm in Sec. II A is applicable for a 2-D signal, while the standard identification algorithms may be generalised at step (iv) by considering the two largest original statistic evaluations instead. Fig. 12 shows plots of discrimination and accurate identification rate against compression for a 2-D signal $\mathcal{S} \propto h_1 + h_2$, compared against a 1-D signal $\mathcal{S} \propto h_1$ with the same true SNR ρ . The identification algorithm I_2 is used, since the accuracy rate of I_1 falls to zero if $m \neq m'$.

For detection of a 2-D GW signal, the effectiveness of the partition scheme is reduced slightly at lower SNR, but mitigated by the case where $m = m'$ (i.e. the higher dotted curves in Fig. 12). The discrimination for a 1-D signal generally lies within the 2-D discrimination bounds; at higher compression rates, there is little to no detection performance lost if the signal is not confined to a 1-D subspace. Accurate identification of a 2-D signal is

more problematic, since accuracy rates are reduced to begin with and fall off rapidly even at high SNR. Nevertheless, options such as lowering compression or switching to $I_{i>2}$ are available for the partition scheme, which should at least allow the template with maximal signal overlap to be identified at acceptable accuracy rates.

If the true SNR is sufficiently high, the standard algorithms $I_{i>j}$ may also be used to identify a j -dimensional GW signal described by an arbitrary linear combination of templates, i.e.

$$\mathcal{S}(t) = \sum_{k=1}^j A_k h_k(t), \quad (47)$$

where $A_k > A_{k+1}$ and the templates have been relabelled without loss of generality. At step (iv) of the algorithms, each ordered weight A_k may be approximated by the k -th largest original statistic evaluation $x_{(k)}$, with the SNR of the identified signal given by

$$\rho_I = \sqrt{\sum_{k=1}^j x_{(k)}^2}. \quad (48)$$

While this method fully recovers the (relative) weights of a GW signal's j largest modes in the limit of infinite true SNR, its accuracy might be severely limited for lower-SNR signals and/or large values of P .

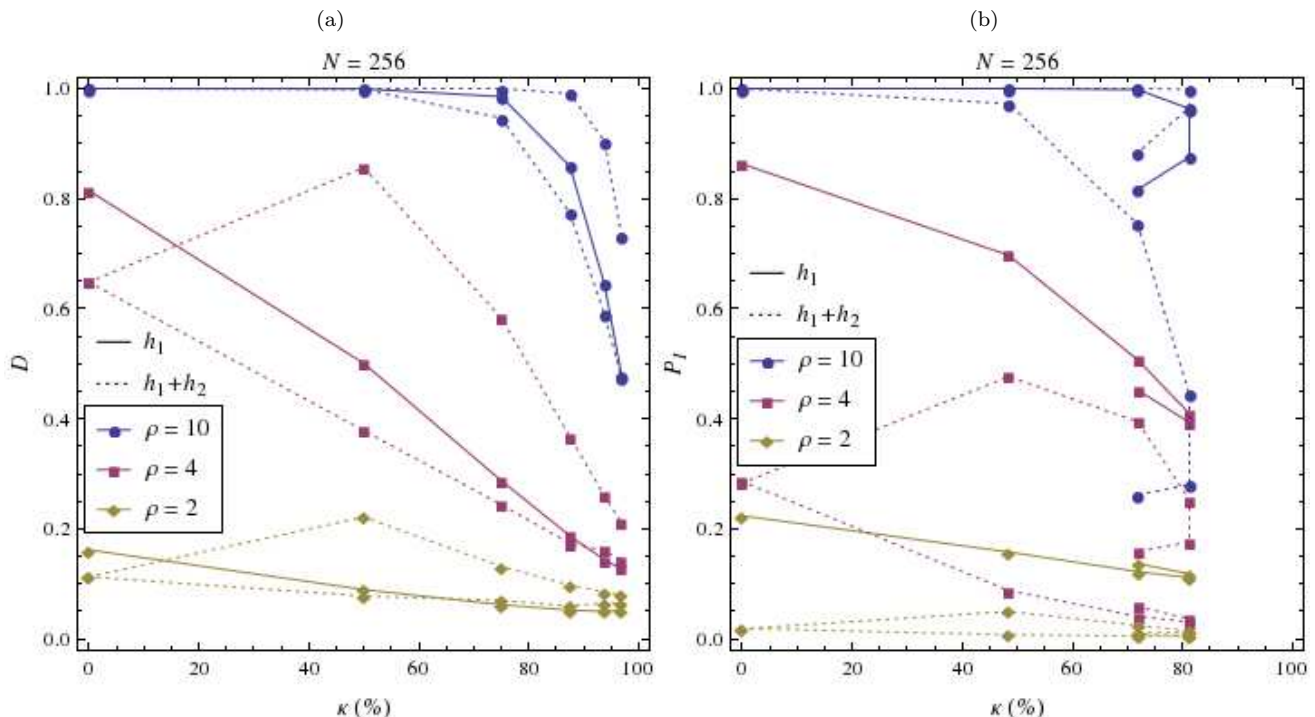


FIG. 12: Plots of (a) discrimination D and (b) accurate identification rate P_I against compression rate κ for the partition scheme with 1-D and 2-D signals, at different values of true SNR ρ for a 256-template bank. The higher dotted curves for each value of ρ correspond to the template labels 1 and 2 being assigned to the same set, while the lower curves correspond to them being assigned to different sets.

V. CONCLUSION

In this paper, we have presented and compared three tunable conic compression schemes that slide between maximal performance and compression for the fast detection and identification of moderate- to high-SNR GW sources.

A recently proposed binary labelling method [17], modified to ensure the equal treatment of templates, is contained as a particular case of the symmetric base scheme. Optimal detection statistics have been calculated for all three schemes under idealised conditions, and the standard maximum-overlap detection statistic is shown to be significantly suboptimal for the two correlated schemes.

While the lossless correlated schemes offer automatic identification of the GW signal upon detection, the benefits of this are negated in the presence of noise. Furthermore, the lossy partition scheme yields better detection and identification performance than its counterparts at the same level of compression; it is also more tunable and scales well with the size of the template bank.

We have implemented the partition scheme for toy models of a non-orthogonal template bank and a GW signal lying in a low-dimensional subspace, to show that it remains feasible under more realistic assumptions. Correlations among the original templates result in highly

partition-dependent performance, but this may be mitigated by selecting an optimised partition beforehand. If the signal is proportional to a linear combination of templates, the detection performance is more variable but not significantly reduced.

In summary, our tunable conic compression schemes—specifically the partition scheme—might provide an effective method of trading detection sensitivity for computational savings in a grid-based search. This is potentially relevant for the source-rich eLISA data sets, where computational costs are more prohibitive and high-SNR sources such as supermassive black-hole binaries are anticipated; for example, it could be used as an online tool to rapidly identify nearby sources before merger and generate alerts for electromagnetic telescopes. Although the method is simplistic, it is fully general and may easily be adapted to supplement existing algorithms in GW data analysis pipelines.

Acknowledgements

AJKC's work was supported by the Cambridge Commonwealth, European and International Trust. JRG's work was supported by the Royal Society.

-
- [1] G. M. Harry (for the LIGO Scientific Collaboration). Advanced LIGO: The next generation of gravitational wave detectors. *Classical and Quantum Gravity*, 27:084006, 2010.
- [2] T. Accadia et al. Status of the Virgo project. *Classical and Quantum Gravity*, 28:114002, 2011.
- [3] G. Hobbs et al. The International Pulsar Timing Array project: Using pulsars as a gravitational wave detector. *Classical and Quantum Gravity*, 27:084013, 2010.
- [4] P. Amaro-Seoane et al. Low-frequency gravitational-wave science with eLISA/NGO. *Classical and Quantum Gravity*, 29:124016, 2012.
- [5] P. Jaranowski and A. Królak. *Analysis of gravitational-wave data*. Cambridge University Press, 2009.
- [6] P. Jaranowski and A. Królak. Gravitational-wave data analysis: Formalism and sample applications. *Living Reviews in Relativity*, 15:4, 2012.
- [7] S. Mitra, S. V. Dhurandhar, and L. S. Finn. Improving the efficiency of the detection of gravitational wave signals from inspiraling compact binaries: Chebyshev interpolation. *Physical Review D*, 72:102001, 2005.
- [8] R. J. E. Smith et al. Towards rapid parameter estimation on gravitational waves from compact binaries using interpolated waveforms. *Physical Review D*, 87:122002, 2013.
- [9] P. Cañizares, S. E. Field, J. R. Gair, and M. Tiglio. Gravitational wave parameter estimation with compressed likelihood evaluations. *Physical Review D*, 87:124005, 2013.
- [10] P. Cañizares et al. Accelerated gravitational-wave parameter estimation with reduced order modeling. 2014. arXiv:1404.6284[gr-qc].
- [11] N. J. Cornish and J. Crowder. LISA data analysis using Markov chain Monte Carlo methods. *Physical Review D*, 72:043005, 2005.
- [12] J. Crowder, N. J. Cornish, and J. L. Reddinger. LISA data analysis using genetic algorithms. *Physical Review D*, 73:063011, 2006.
- [13] F. Feroz, J. R. Gair, M. P. Hobson, and E. K. Porter. Use of the MULTINEST algorithm for gravitational wave data analysis. *Classical and Quantum Gravity*, 26:215003, 2009.
- [14] I. S. Heng. Rotating stellar core-collapse waveform decomposition: A principal component analysis approach. *Classical and Quantum Gravity*, 26:105005, 2009.
- [15] K. Cannon et al. Singular value decomposition applied to compact binary coalescence gravitational-wave signals. *Physical Review D*, 82:044025, 2010.
- [16] S. E. Field et al. Reduced basis catalogs for gravitational wave templates. *Physical Review Letters*, 106:221102, 2011.
- [17] Y. Wang. Fast detection and automatic parameter estimation of a gravitational wave signal with a novel method. 2014. arXiv:1402.6217[gr-qc].
- [18] S. V. Dhurandhar and B. S. Sathyaprakash. Choice of filters for the detection of gravitational waves from coalescing binaries, II: Detection in colored noise. *Physical Review D*, 49:1707, 1994.
- [19] T. A. Apostolatos. Search templates for gravitational waves from precessing, inspiraling binaries. *Physical Review D*, 52:605, 1995.
- [20] B. J. Owen. Search templates for gravitational waves from inspiraling binaries: Choice of template spacing. *Physical Review D*, 53:6749, 1996.
- [21] N. L. Biggs. *Discrete mathematics*. Oxford University Press, 2002.
- [22] R. C. Bose. On the application of the properties of Galois fields to the problem of construction of hyper-Graeco-Latin squares. *Sankhyā: The Indian Journal of Statistics*, 3:323, 1938.
- [23] C. W. H. Lam, L. Thiel, and S. Swiercz. The non-existence of finite projective planes of order 10. *Canadian Journal of Mathematics*, 41:1117, 1989.
- [24] D. Singmaster. How often does an integer occur as a binomial coefficient? *American Mathematical Monthly*, 78:385, 1971.
- [25] D. Singmaster. Repeated binomial coefficients and Fibonacci numbers. *Fibonacci Quarterly*, 13:295, 1975.
- [26] B. S. Sathyaprakash and S. V. Dhurandhar. Choice of filters for the detection of gravitational waves from coalescing binaries. *Physical Review D*, 44:3819, 1991.
- [27] S. V. Dhurandhar and B. F. Schutz. Filtering coalescing binary signals: Issues concerning narrow banding, thresholds, and optimal sampling. *Physical Review D*, 50:2390, 1994.
- [28] The curves for (23) were obtained via 10^5 -trial Monte Carlo simulations, while numerical integration of (16) and (17) was used to generate quicker and more precise curves for (24).
- [29] The covariance matrix defined by (29) is rank-deficient, but we may take the Moore–Penrose pseudoinverse Σ^+ as a suitable (perturbative) approximation to Σ^{-1} in (12) and (13).